Proceedings of the Seventh IASTED International Conference
POWER AND ENERGY SYSTEMS
August 29–31, 2007, Palma de Mallorca, Spain
ISBN Hardcopy: 978-0-88986-689-8 / CD: 978-0-88986-690-4

HIGH EFFICIENCY CONTROL OF A GRID CONNECTED PV CONVERTER

Attila Balogh*, Zoltán Tamás Bilau[+] and István Varjasi*
Budapest University of Technology and Economics
Department of Automation and Applied Informatics*
Exendis-Deltronic Kft.[+]
Budapest Goldmann Gy. Square 3*, Ilka street 47[+]
Hungary
balogh@aut.bme.hu, z.bilau@exendis.com, varjasi@aut.bme.hu

ABSTRACT
The efficiency of the converter is one of the most important parameters of a grid connected PV system, since the price of PV cells is still very high. One possible method of increasing the efficiency is constructing a power circuit without transformer. For avoiding EMC problems in this case we need not only differential mode, but also common mode filter at the DC-AC converter. Just connecting the middle point of the DC capacitive filter to the neutral line of the grid, the high frequency current between the PV array and the grid become acceptable, but the ripple current in the filtering AC inductance become somewhat higher. As the major part of core-loss caused by the ripple current, this will decrease the efficiency especially at low power (i.e. at low radiation). The proposed control method will decrease the ripple current, hence significantly improve the efficiency in the low power operating domain. With the proposed 3SC (Three State Control) method each leg of the inverter have 3 possible states (high on, low on, both off) unlike the 2 states at the traditional control method.

KEY WORDS
High efficiency, 3 state control, photovoltaic converter, control strategy.

1. Introduction

Nowadays in applications of renewable energy sources it is important to develop powerful and energy-saving photovoltaic converters and to keep the prescriptions of the standards. The improved efficiency of PV converters and the decreasing price of PV cells lead to the widespread u tilization of this kind of renewable energy [1]. Last years depending on PV converter type there were some software and hardware [2][3][4][5] solutions for increasing the efficiency.

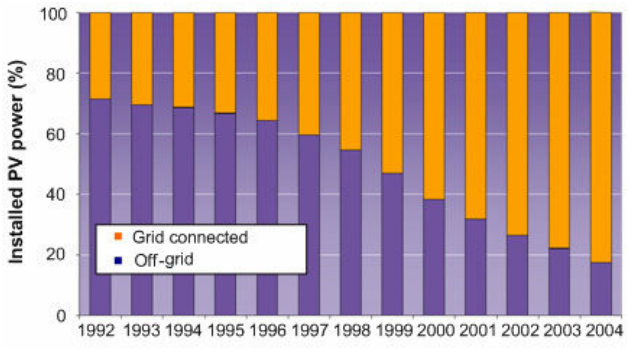

Fig. 1.Installed PV power in percentage during last decade in IEA PVPS reporting countries (source: IEA-PVPS).

The average prices for PV modules are around €5/Wp in Europe, but the best price could be as low as €3/Wp for monocrystalline and polycrystalline modules and €2.5/Wp for thin film modules.
The prices of PV cells in the last years are shown in Fig. 2.

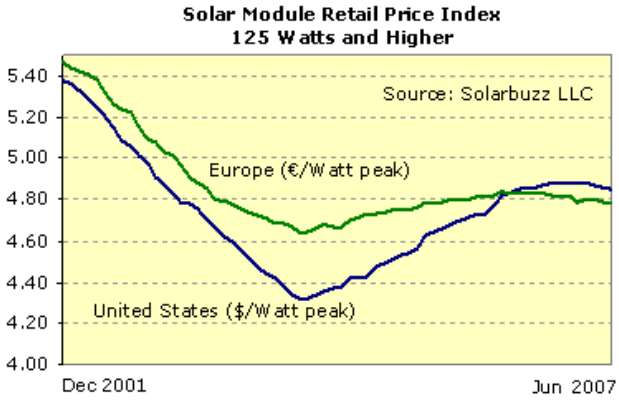

Fig. 2. Photovoltaic module prices from Dec. 2000 to Jun 2007.

In addition to the PV module cost (see Fig.2.), the cost and reliability of PV inverters are basic issues when market competitive PV supply systems are the aim. The inverter cost represents about 10-15% of the total investment cost of a grid connected system. The development of PV inverter in small to medium power range the inverter cost of this power class has decreased by more than 50% during the last 10 years. The main reasons for this reduction are the increase of the production quantities and the implementation of new system technologies.

From Fig.2. it can be seen, that nowadays the photovoltaic arrays are pretty expensive yet, so the ratio of the cell/converter price has not been changed significantly. This also means, that 1% improvement of the efficiency causes about 10% more valuable converter. The most frequent main circuit arrangement is the three phase bridge [6][7][8][9][10][11][12]. When a transformer is used for galvanic isolation, we have some freedom for the common mode voltage of the converter. In this case the efficiency can be improved by the flat-top or discontinuous PWM [13]. A further improvement may be reached at low radiation utilizing the 3SC as described in [14][15]. As in the EU standard the galvanic isolating transformer is not mandatory anymore see abstract [16]. The main advantage of our method is, that it is unnecessary to change the aforementioned topology of the converter, only the modification of the control is needed. In this paper we will introduce an algorithm developed for single phase converters.

2. Structure of the photovoltaic converter

The first part of the power circuit is the PV array, which converts the solar energy into DC power. An optional step-up converter (Fig.3, Boost DC/DC converter) may raise the voltage level of the PV array to the one of the three-phase IGBT bridge. The control of the boost chopper algorithm includes the maximal power point tracking (MPPT). The MPPT together with the input filter of the chopper ensures the maximal utilization of the array. The boost chopper is unnecessary when the voltage of the array at MPP is greater than the voltage necessary for sinusoidal AC current control. The three-phase bridge converts the DC voltage to nearly sinusoidal AC currents. This topology can be used with and without output transformer. In the US the output transformer is mandatory but in the EU it is optional [16]. In the followings we consider the case, where the converter is connected through low-pass filter to the grid, without a transformer.
The high order harmonics of the output current are filtered out by passive L-C-L-C low-pass filter (see Fig.4). The L_2-C_2 low-pass filter has higher cut-off frequency than L_1-C_1 has so U_g' can be approximated by U_g.. On the DC side L_3 can be omitted when the optional boost converter exists. The DC component of U_{d1} and U_{d2} is controlled to equal values through the DC component of the neutral line's current (which is zero in stationary state). At symmetrical grid voltage the AC part of U_{d1} and U_{d2} consists of switching frequency (and above) components and are negligible. In stationary state $U_{d1} = U_{d2} = U_b/2$.

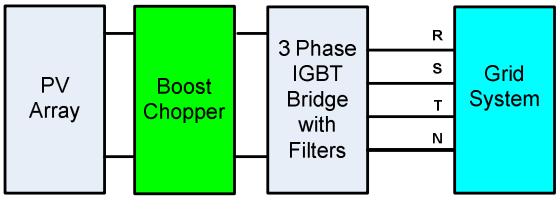

Figure 3. Structure of the power circuit

With this arrangement the voltage between any point of the PV array and the earth will be relatively low, i.e. close to, or less than the peak phase voltage of the grid. The control is easier, since the three phase converter control equals to three single phase converter control. The high order harmonic content of the PV array current is negligible. This arrangement has one small drawback. With conventional control some high order current harmonics appear on the output [17]. As the core-loss of the inductances is independent from the actual power, this will decrease the efficiency especially at low power (e.g. at 10% radiation). The new developed control method reduces this harmonics content through the 3 state control method. With this current control method the efficiency of the converter could be gained in a phase, where the instantaneous current reference is lower than the ripple current of the first stage (L_1) of the AC filter.

3. Current control

The current control mode depends on the current of the L_1 output inductance and on the voltage of the DC link and the grid. There are two modes, the traditional continuous and the 3 state control.

3.1 Continuous current mode

In continuous current mode at stationary-state the current on the L_1 output inductance do not reaches the zero level at the actual T_c switching period. (Fig.5.)

While the higher switch is on the voltage on the L_1 output inductance is the difference between the high side of the DC link and the C_1 filter capacitance voltage (approximated by the grid voltage). The current ripple of the inductance is:

$$\Delta I_L = \frac{U_L}{L_1} T_{on} = \frac{U_{d1} - U_g}{L_1} T_{on}, \qquad (1)$$

where U_g is the phase voltage of the grid, U_{d1} is the voltage of the high side DC link, L_1 is the output filter inductance, and T_{on} is the switching-on time of the IGBT.

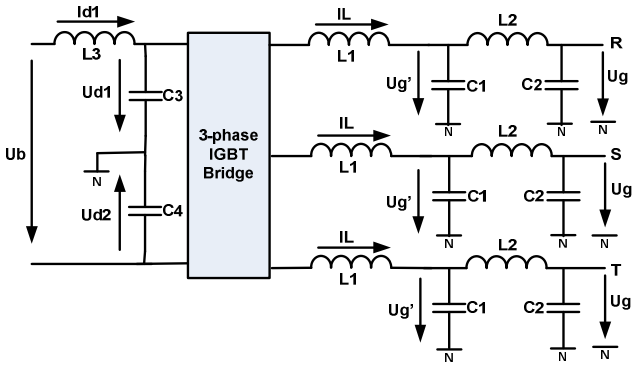

Figure 4. The IGBT bridge with the filters

When the high side IGBT is turned on, the output voltage of the converter is U_{d1}, while in the opposite case the output voltage is U_{d2}.

If the change of the current reference (I_{ref}) during the PWM period (T_c) is negligible, there is a voltage balance on the two sides of L_1:

$$U_g \approx \frac{T_{on}U_{d1} + T_{diode}U_{d2}}{T_c}, \qquad (2)$$

where T_{diode} is the switching-on time of the diode.

Furthermore if U_{d1} is equal to $-U_{d2}$ (2) may be approximated as:

$$U_g \approx \frac{2T_{on}U_{d1} - T_cU_{d1}}{T_c}. \qquad (3)$$

From (3) the switching-on time for stationary state is:

$$T_{on} = \frac{T_c}{2}\left(\frac{U_g}{U_{d1}} + 1\right). \qquad (4)$$

After substitution of (4) in (1) the current ripple is:

$$\Delta I_L = \frac{T_c * U_{d1}}{2L_1}\left[1 - \left(\frac{U_g}{U_{d1}}\right)^2\right]. \qquad (5)$$

It is seen, that at every grid voltage-peak the current ripple is the smallest, where U_g has the largest absolute value. For the grid-connected inverters the power-factor is close to 1 (should be above 0.95). The current is just maximal at the smallest current ripple, so the current mode in that domain is always continuous [14].

Unlike with traditional controllers we control directly not the average, but the peak value of the current in every switching period. The current reference is derived from the output of the voltage controller multiplied by the sinus of the identified phase angle [15]. The result means average value, which should be corrected by the ripple current for the current-peak reference. The current-peak reference in the next PWM period depends on the current reference, on the grid voltage and on the DC link voltage:

$$I_{Lm}(I_{ref}, U_g, U_{d1}, U_{d2}) = I_{ref} + \frac{\Delta I_{Lnom}}{2}, \qquad (6)$$

where ΔI_{Lnom} is the estimated current ripple of the output inductance, I_{Lm} is the next current-peak reference and I_{ref} is the reference current.

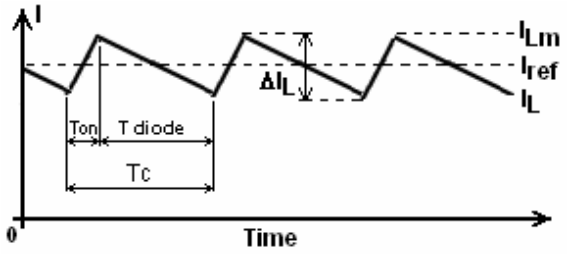

Figure 5. Continuous current waveform

The estimated current ripple of the output inductance is:

$$\Delta I_{Lnom} = \frac{U_d - U_g}{L_1}T_{onn}. \qquad (7)$$

From (2) - if the average voltage of the inductance is zero - the nominal switching-on time (T_{onn}) is:

$$T_{onn} = T_c * \frac{U_{d1} - U_g}{U_{d1} - U_{d2}}. \qquad (8)$$

In every PWM period we measure the peak current of the output inductance. With appropriately calculated T_{on} the next current-peak reference (calculated from (6)) can be reached in one switching period:

$$I_{Lm} = I_{L[n]} + \frac{(T_c - T_{on})(U_{d2} - U_g) + T_{on}(U_{d1} - U_g)}{L_1}, \qquad (9)$$

where $I_{L[n]}$ is the actual measured current peak.

From (9) the next switching-on time ($T_{on[n+1]}$) of the transistor is:

$$T_{on[n+1]} = \frac{\left(I_{Lm} - I_{L[n]}\right)L_1 - T_c\left(U_{d2} - U_g\right)}{U_{d1} - U_{d2}}, \qquad (10)$$

where U_{d2} is the voltage of the low side DC link.

The duty cycle can determined from the result of (10):

$$d = \frac{T_{on[n+1]}}{T_c}. \qquad (11)$$

3.2 3 state control

We can switch to 3 state control, when the stationary-state current of the output inductance with traditional control would cross the zero level. In this case we can add another degree of freedom to the control. We may reach the current reference with less ripple current, if we control only the IGBT according to the direction of current reference. The result is the discontinuous current mode with less input current but with the challenge of nonlinear control (see Fig. 6).

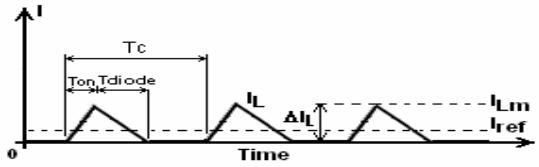

Figure 6. Discontinuous current waveform

At every zero crossing of the grid voltage (U_g) the current ripple (5) would be the highest using traditional continuous mode control and the current reference is near zero. The current mode in this domain is always discontinuous with 3 state control.

In discontinuous current mode the average current of one switching cycle should also be equal to the reference:

$$I_{ref} = \frac{(T_{on[n+1]} + T_{diode}) * I_{Lm}}{2 * T_c}. \quad (12)$$

The switching-on time of the diode can be approximated as:

$$T_{diode} = I_{Lm} * \frac{L_1}{U_{d2} - U_g}. \quad (13)$$

The peak current of the IGBT from the switching-on time:

$$I_{Lm} = \frac{U_{d1} - U_g}{L_1} T_{on}. \quad (14)$$

After substitution of (13) in (12):

$$T_{on[n+1]} = \frac{2T_c I_{ref}}{I_{Lm}} - \frac{I_{Lm} L_1}{U_{d2} - U_g} \quad (15)$$

After substitution of (14) in (15) and solved the equation the next switching-on time in discontinuous mode is:

$$T_{on[n+1]} = \sqrt{A^2 + B} - A, \quad (16)$$

where A and B are as following:

$$A = \left[\frac{(U_{d2} - U_g) I_{Lm} L_1}{2(U_{d1} - U_g)^2} \right] \quad (17)$$

$$B = \left[\frac{2 L_1 I_{ref} T_c (U_{d2} - U_g)}{(U_{d1} - U_g)^2} \right]. \quad (18)$$

From (16) the discontinuous duty cycle is:

$$d^* = \frac{T_{on[n+1]}}{T_c}. \quad (19).$$

In every PWM period the controller calculates both the continuous and discontinuous duty cycle.

There are two cases: in the first one the current mode is discontinuous, so the discontinuous duty cycle is smaller than the continuous one. In the second case at continuous current mode the controller calculates the discontinuous duty cycle and it is bigger than the PWM period. This means that the current mode is continuous, so the real duty cycle is always the smaller one.

4. Experimental results

The experimental results were carried out on an EXENDIS DELTRONIC PSDC700/30 frequency-converter with a nominal power of 10kW. The chokes of the filter have 700uH inductance. The switching frequency was 16.5 kHz.

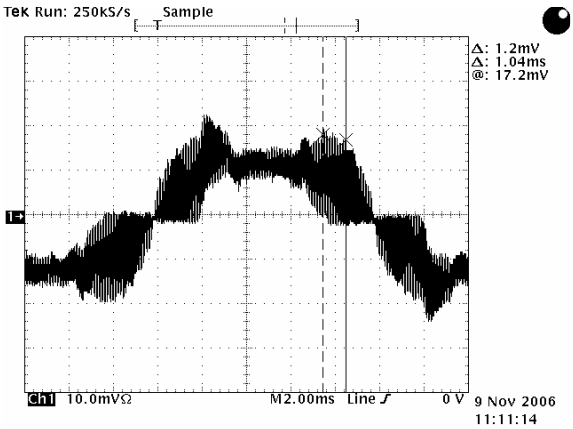

Figure 7 Current of the output inductance at nominal load (measurement)

According to Fig. 4 in discontinuous mode the current of the output inductance changes between the reference and the zero level. It is seen, that the device was in almost half of the time in the discontinuous current mode (see Fig. 7).

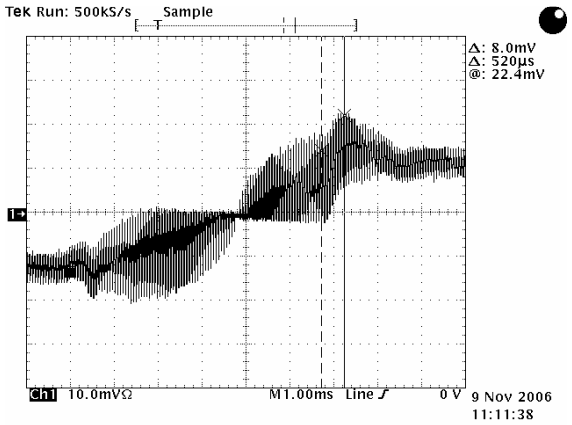

Figure 8. Current of the output inductance at nominal load about the zero cross (measurement)

With the traditional continuous current control the current ripple at zero-cross of U_g would be the maximal. With the developed 3 state control the ripple current is just zero at that time. After the zero cross of U_g the ripple current increases according to a square root function of time until the current of the continuous mode reached (see Fig. 8).

4.1 Comparison of 3SC with the traditional current control

In this subsection the comparison of the 3SC and the traditional control is presented. In the Figure 9 the output current of the PV converter at 10% of nominal load with traditional sinusoidal control, while in Figure 10 with the new developed control method can be seen. With the traditional control the output current cyclic changes between positive and negative values causing significant switching and iron losses, while with 3SC the current changes between positive and zero and between negative and zero values. The harmonic content of the output current become significant at small load, so we will investigate the currents at 10% and at 35% of nominal load.

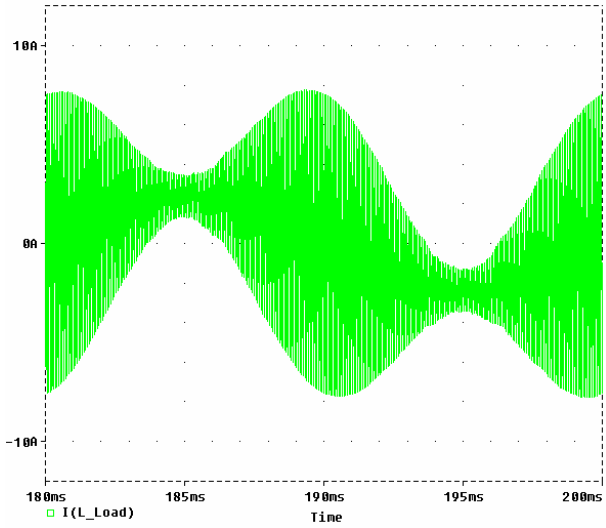

Figure 9. Output current with traditional control at 1kW power (simulation)

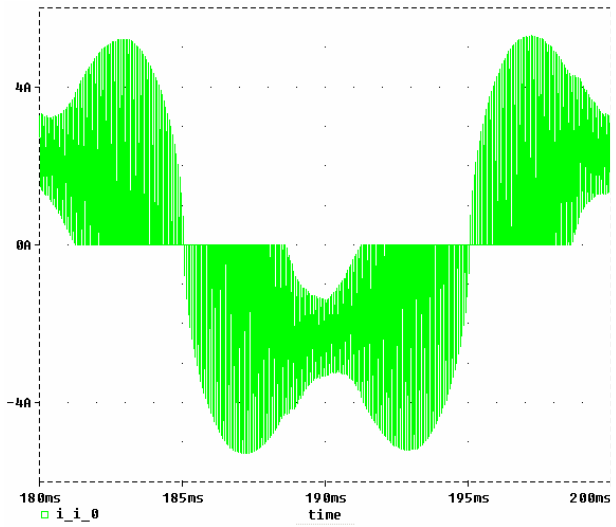

Figure 10. Output current with 3SC at 1 kW power (simulation)

In the Figure 11 and 12 also the output current can be seen at 35% of nominal load with traditional and 3SC. Due the greater load the harmonic content compared to the base harmonic is smaller.

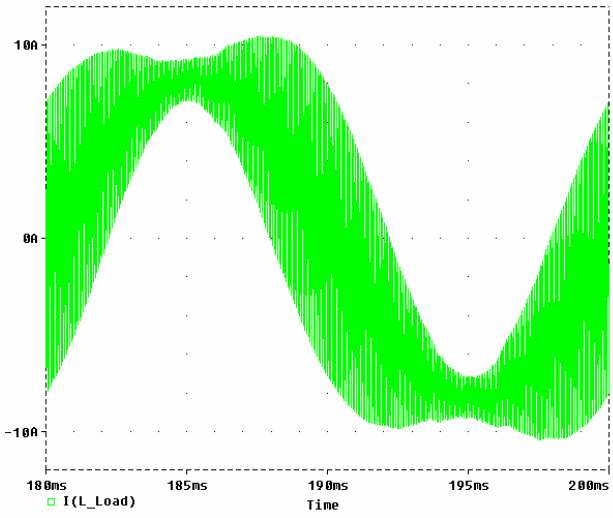

Figure 10. Output current with traditional control at 3.5kW power (simulation)

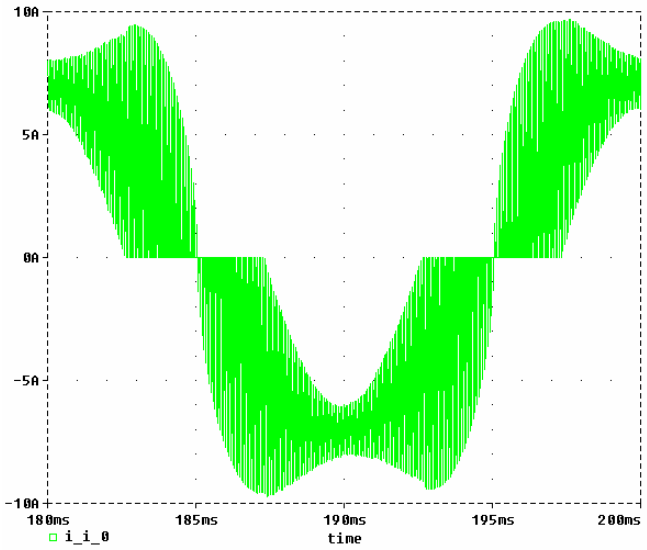

Figure 11. Output current with 3SC at 3.5kW power (simulation)

In Table 1 the switching harmonic currents can be seen at the given switching frequency. It can be seen, that with the new control method the iron losses of the grid side inductors would be smaller and the switching-on losses of the IGBT-s would be zero and the switching-off losses would be also smaller.

Load	Mode	16.5kHz	33kHz	49.5kHz
1kW	Traditional	3.8032	1.0189	0.435
	3 state	1.4575	0.7243	0.428
3.5kW	Traditional	3.8022	1.0189	0.435
	3 state	2.4718	0.9889	0.4872

Table 1. Harmonic currents at 16.5 kHz switching frequency

5. Conclusion

With the proposed control method on the presented topology a high performance (high efficiency) converter was obtained even in the low radiation (less than 10% of nominal) operating mode.

Acknowledgements

The research was supported by the Economic Competitiveness Operative Program (GVOP 3.3 project for "Modular energy converters for railway …") for which authors express their sincere gratitude.

References

[1] Dr.Mike Meinhardt, Gunter Cramer, Past, Present and Future of grid connected Photovoltaic- and Hybrid-PowerSystems, IEEE 2000.

[2] P. Wood, "Switching Power Converters," Van Nostrand Reinhold Company, New York, 1981.

[3] H. W. van der Broeck, H. Ch. Skudelny, and G. Stanke," Analysis and realization of a pulse width modulator based on voltage source space vectors," IEEE Transactions on Industrial Applications, vol 24 , pp 142-150, 1988.

[4] S. Ogasawara, H. Agaki, and A. Nabae," A novel PWM scheme of voltage source inverter based on space vector theory," Conference record European Power Electronics Conf., pp 1197-1202, 1989.

[5] G. Buja and G Indri," Improvement of pulse width modulation techniques," Arch Elektrotech. (Germany), vol 57, pp 281-289, 1975.

[6] T. Shimizu, M.Hirakata, T. Kamezawa, H. Watanabe, „Generation Control Circuit for Photovoltaic Modules" IEEE Trans. On Power Electronics, Vol. 16, No. 3, May, 2001, pp. 293

[7] R.W. Erickson, D. Maksimovic, "Fundamentals of Power Electronics", Kluwer Academic Pub; March 1, 1997, ISBN: 0-412-08541-0, 773 pages.

[8] M. Calais, J. Myrzik, T. Spooner, V.G. Agelidis, "Inverters for single-phase grid connected photovoltaic systems-an overview", Proc. of PESC '02, 2002, Vol. 4, pp. 1995 – 2000

[9] R. Teodorescu, F. Blaabjerg, M. Liserre, U. Borup, " A New Control Structure for Grid-Connected PV Inverters with Zero Steady-State Error and Selective Harmonic Compensation", Proc. of APEC'04, , Vol. 1, 2004, pp. 580-586.

[10] F. Blaabjerg, R. Teodorescu, Z. Chen, M. Liserre, "Power Converters and Control of Renewable Energy Systems", Proc. Of ICPE'04, 2004.

[11] H. Haeberlin, "Evolution of Inverters for Grid connected PV systems from 1989 to 2000", Proc. of Photovoltaic Solar Energy Conference, 2001.

[12] J. Rodriguez, J. Dixon, J. Espinoza, P. Lezana, PWM regenerative rectifiers IEEE Transaction on Ind. Electronics, state of the art, vol.52, Chile, February 2005.

[13] Ahmet M. Hava, Russel J. Kerkman, Thomas A. Lipo, A High-Performance Generalized Discontinuous PWM algorithm, IEEE transaction on indiustry applications, vol 34, 1998.

[14] A. Balogh, I. Varjasi, Discontinuous Current Mode of a Grid Connected PV Converter, IYCE2007, Budapest, Hungary

[15] I. Varjasi, A. Balogh, S. Halasz, Sensorless control of a grid connected PV converter, EPE-PEMC2006, Portoroz., Slovenia.

[16] UL 1741, UL Standard for inverters, converters, and controllers for use in independent power production systems, Northbrook, 2001

[17] IEC 61727 International Standard, Photovoltaic (PV) systems – Characteristics of the utility interface, Switzerland, 2004.